

STUDY OF CHARGE DENSITY, DENSITY OF STATES AND ELECTRON MOMENTUM DENSITY OF ZnS_xSe_{1-x} SEMICONDUCTOR ALLOYS

C.B. SWARNKAR, R.K. PANDYA^a, U. PALIWAL^b, N.N. PATEL^{b,s}, K.B. JOSHI^{b,*}

Department of Physics, S.G.G. Govt. (PG) College, Banswara-327001 (India).

^aDepartment of Physics, L.B.S. (PG) College, Jaipur-302004 (India)

^bDepartment of Physics, University College of Science, ML Sukhadia University, Udaipur-313001 (India)

Electronic properties of semiconducting ZnS_xSe_{1-x} alloys following empirical pseudopotential method are presented in this work. Alloying effects are considered through modified virtual crystal approximation. Calculations are performed for the semiconducting alloys ZnS_xSe_{1-x} (with $x=0.0, 0.25, 0.50, 0.75$ and 1.0) to report refractive index, bowing parameter b for E_{Γ_1} , charge density, electronic density of states and the electron momentum density distribution. Charge density distributions along the cation, anion and the bond intersecting planes are presented. For all alloys simulated total density of states are discussed to examine the effect of alloying. Effect of alloying is also examined on the electron momentum densities of the alloys. The calculated bowing and refractive indices are found to be in good agreement with the experimental reports. Trends in ionicity factors support the signatures of charge transfer on the basis of charge density also. Study on electron momentum distributions indicates that in the low momentum region substitution of Se in ZnS gives rise to increase in momentum densities.

(Received March 23, 2009; accepted March 31, 2009)

Keywords: Bowing parameter, Charge density, Density of States, Empirical Pseudopotential Method, Electron momentum distribution, II-VI ternary semiconducting alloys.

1. Introduction

The II-VI wide band gap semiconducting alloys have applications in fabricating technologically important solid state devices [1,2]. The ZnS_xSe_{1-x} semiconducting alloys are used to fabricate optoelectronic devices ranging from infrared to ultraviolet (UV) radiation [3]. Due to variation in band gap with composition, these are highly suitable to fabricate wavelength tunable UV-photodiodes [4]. Also the direct band gap over entire composition range ($0 \leq x \leq 1$) enables its usage in visible laser diodes, light emitting diodes (LEDs) and bright light emitters [1].

The II-VI mixed-anion semiconductor alloys are studied relatively less than the mixed-cation alloys both from theoretical methods and experimental techniques. A few theoretical models have been applied on ternary alloys and the binary compounds. For instance, Homann et al [5] applied linear combination of atomic orbitals (LCAO) method to report electronic and structural properties of ZnS_xSe_{1-x} alloys over entire composition range. On the basis of EPM, Nasrallah et al [6] reported the electronic structure and band offsets of ZnS_xSe_{1-x} alloys and heterostructures. A semi empirical MSINDO method was applied by Janetzko and Jug [7] to compute binding energies, entropy of mixing and miscibility of ZnS_xSe_{1-x} . The quasi particle scheme was applied by Fitzer et al [8] for ZnS and ZnSe. A gradient corrected hybrid scheme was employed to report

*Corresponding author: cmsmlsu@gmail.com.^s Now at OCES-BARC, Mumbai

band gap for a number of materials including ZnS by Muscat and coworkers [9]. Bernard and Zunger [10] reported the band gap and related properties of $\text{ZnS}_{0.5}\text{Se}_{0.5}$ using plane wave method based on local density approximation (LDA).

Only a few experimental studies of the $\text{ZnS}_x\text{Se}_{1-x}$ alloys are reported. The difficulty posed by miscibility in forming the solid state might probably be the reason for paucity of experimental studies. Nevertheless, very recently Homann et al [5] reported band gap for all compositions applying optical spectroscopy. Theis [11] reported experimental band gap for the binary compounds ZnS and ZnSe. Ebina et al [12] reported reflectivity measurements and indicated that $\text{ZnS}_x\text{Se}_{1-x}$ alloys are amalgamation type.

Table 1. Band gaps calculated for $\text{ZnS}_x\text{Se}_{1-x}$ semiconductor alloys employing the EPM method within the MVCA. The LCAO calculations have been performed by Homann et al [5] using ab-initio CRYSTAL code. The measurements reported by Ebina et al and Homann et al are at room temperature.

	Band gap E_g (eV)				
	Theory		Experiment		
	This work	LCAO [5]	Van de Walle [32]	Ebina et al [12]	Homann et al [5]
ZnSe	2.77	3.0	2.82	2.72	2.58
$\text{ZnS}_{0.25}\text{Se}_{0.75}$	2.99	3.18	----	2.85	2.73
$\text{ZnS}_{0.50}\text{Se}_{0.50}$	3.21	3.29	----	3.08	2.92
$\text{ZnS}_{0.75}\text{Se}_{0.25}$	3.47	3.47	----	3.34	3.17
ZnS	3.85	3.68	3.78	3.70	3.45

To examine suitability of materials one needs to study nature and characteristics of electronic states and bonding. *Ab-initio* methods based on the LDA and other approximation schemes like generalized gradient approximation (GGA) within the density functional theory (DFT) give diverging estimates of the band gap and related properties especially for the semiconductors alloys [11,13]. It is worth emphasizing that for quaternary alloys full potential linearised augmented plane wave (FP-LAPW) method coupled with the tight binding (TB) method has shown deviation from the experimental band gap and bowing [14]. The **k.p** method and the quasi particle scheme are the other methods applicable for semiconductors [15]. However **k.p** method has received theoretical criticism owing to violation of low momentum assumption in the perturbation [16]. A number of theoretical calculations performed on $\text{ZnS}_x\text{Se}_{1-x}$ alloys to report band gaps and bowing parameters show diverging results [5-7,14]. Thus, bowing deduced from all these calculations are inconsistent and deviate from experimental results. Empirical pseudopotential method (EPM) is also a reliable and rapidly converging method. It is relatively easy to deal with large number of plane waves in this method. The residual ambiguities in this method have been improved by adopting the modified virtual crystal approximation (MVCA) [17]. The band structure thus obtained can be used to quantify degree of covalence on the basis of various proposed scales [18]. The method can also be employed to calculate refractive index, ground state properties like electron momentum density [19] and charge densities [20]. To our knowledge, it may probably be the first attempt to report charge density and density of states for $\text{ZnS}_x\text{Se}_{1-x}$ alloys. It is worthy to note that study of electron momentum density distribution in solids is also one of the important modes to unravel electronic structure. It can be studied theoretically while deriving bonding electron wave functions in momentum space and experimentally by electron momentum spectroscopies like inelastic X-ray scattering [21] or the gamma-ray Compton scattering [22] and the 2 dimensional angular correlation of annihilation

radiation (2D-ACAR)[22] spectroscopy. The 2D-ACAR requires highly pure samples as low atomic concentration is a serious issue in the determination of momentum density in substitutional alloys unlike inelastic X-ray or the gamma ray Compton scattering. So far, to our knowledge, momentum density distribution of bonding electrons in ternary or quaternary semiconductor alloys have hardly been attempted. It may primarily be due to treatment of the alloying effects leading to diverging band gap estimates, miscibility in forming solid state and sensitivity of the positron in determining momentum density distribution around substitution site. Therefore, in this work we also report electron momentum distribution in II-VI ternary $\text{ZnS}_x\text{Se}_{1-x}$ alloys. In this comprehensive study we also report estimates of ionicity, bowing parameter and the refractive index for practical applications. The computed quantities are compared with available theoretical and experimental data for critical analysis. The paper is organized as follows: in second section we briefly describe the method of calculation. In III section, we discuss and present our results on electronic states, bowing, refractive index; charge density and ionicity; density of states and electron momentum density. The fourth section is devoted to conclude findings of this work.

2. Method and computation details:

EPM is based on the form factors which are obtained by fitting energy gaps to available highly reliable experimental data. The crystal potential $V(\mathbf{r})$ is generated by superposition of individual atomic potentials described by the corresponding form factors. Basic formulation employed to implement the calculation of band structure for II-VI alloys can be found elsewhere [20,23]. The crystal potential for an alloy is generated applying virtual crystal approximation (VCA). VCA reasonably describes the bands and bonds in semiconducting alloys with small lattice mismatch [24]. As VCA neglects the interaction between constituents responsible for the disorder, the interaction is included in the modified virtual crystal approximation (MVCA) by introducing a disorder parameter (p) [17,24]. In the MVCA, the alloying potential is described as:

$${}^{\text{MVCA}}V_{\text{ZnSSe}}(\mathbf{G}) = {}^{\text{VCA}}V_{\text{ZnSSe}}(\mathbf{G}) - p[x(1-x)]^{1/2} (V_{\text{ZnS}}(\mathbf{G}) - V_{\text{ZnSe}}(\mathbf{G})), \quad (1)$$

where x is the concentration of sulfur, \mathbf{G} is the reciprocal lattice vector and the VCA describes potential under simple virtual crystal approximation [25].

To quantify ionicity in bonded semiconductors, a number of empirical scales are proposed [18,26-28]. On the basis of heteropolar gap, E_h , Al Douri et al [26] have proposed the following scale for ionicity factor, f_i :

$$f_i = 0.91 - \left(\frac{2}{E_h} \right). \quad (2)$$

Here E_h is the heteropolar gap. We have followed the prescription of Al Douri et al [26] to compute the ionicity for $\text{ZnS}_x\text{Se}_{1-x}$ alloys.

Table 2. Refractive index (n) computed for the alloys following the relation of Moss [34], Herve and Vandemme (HV)[35] and Gupta and Revindra (GR)[36].

Material	Theory			Experiment [41]
	Moss	HV	GR	
ZnSe	2.42	2.42	2.36	2.5
$\text{ZnS}_{0.25}\text{Se}_{0.75}$	2.37	2.35	2.23	-
$\text{ZnS}_{0.50}\text{Se}_{0.50}$	2.33	2.29	2.09	-
$\text{ZnS}_{0.75}\text{Se}_{0.25}$	2.29	2.22	1.93	-
ZnS	2.23	2.12	1.69	2.36

To perform calculations, the available potential parameters used for ZnSe and ZnS were further optimized to construct the pseudopotential for the crystal Hamiltonian. The lattice constants for the alloys were calculated using the Vegards'law [29] and the potential was generated under the MVCA [6,17,18] taking fitted disorder parameter $p=0.357$. About 400 plane waves were considered to generate basis to explore electronic properties. The total charge density was found to be normalized to the degree of 1 part in 10^5 . To compute the momentum density in terms of Compton profile the Fourier inversion scheme of Pattison et al [30] is applied. The details of the scheme can be found elsewhere [19]. To compute the \mathbf{k} summation within the Brillouin zone, special points scheme of Chadi and Cohen [31] was employed. The convergence in autocorrelation functions was ensured by observing accuracy of 1 part in 10^4 at $r=30$ a.u.

3. Results and discussion:

3.1. Electronic states, bowing and refractive index:

Electronic band structures of $\text{ZnS}_x\text{Se}_{1-x}$ for $x=0.0, 0.25, 0.50, 0.75$ and 1.0 are calculated using VCA as well as MVCA. The conduction band minimum and the valence band maximum for the entire range remains at the Γ point. The computed band gaps for all compositions are summarized in table 1. To determine bowing parameter b for E_Γ , we have fitted a nonlinear curve to the band gaps calculated for a number of compositions. The calculated bowing $b=0.4$ eV is in good agreement with the experimental bowing $b=0.35$ eV reported by Homann et al [5] and 0.43 eV by Nicholls et al [33]. It is worth noting that our results get reconcile with measurement better than that of Rabah et al [14] who reported 0.63 eV employing FP-LAPW scheme within the TB method. It indicates that disorder effects are well described by the MVCA in $\text{ZnS}_x\text{Se}_{1-x}$ alloys.

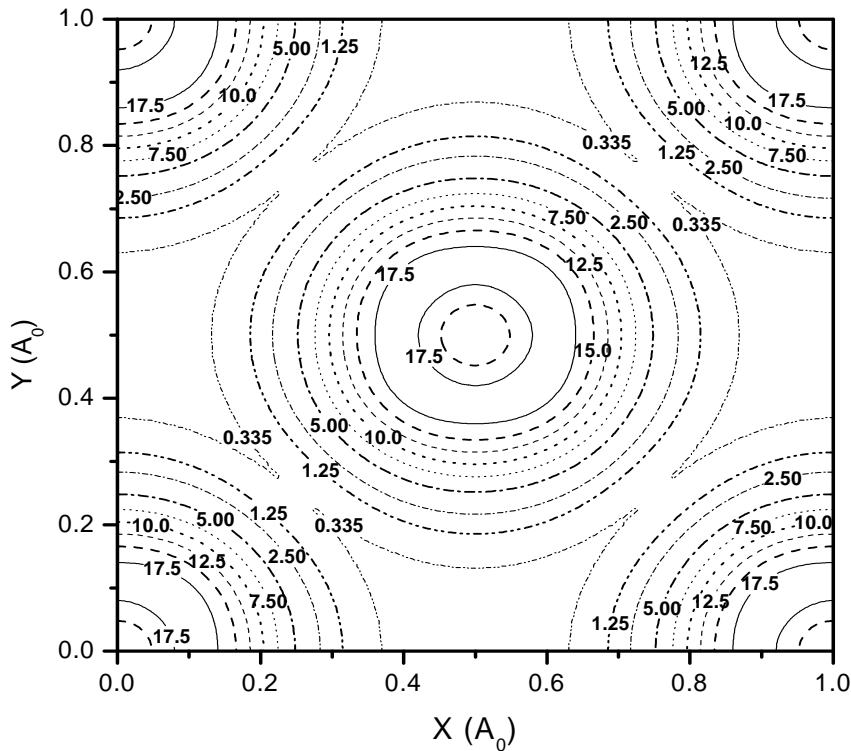


Fig. 1: Electron charge density ($e/a.u.^2$) of valence bands at $z=0.0$ plane for $\text{ZnS}_{0.25}\text{Se}_{0.75}$ at Γ point.

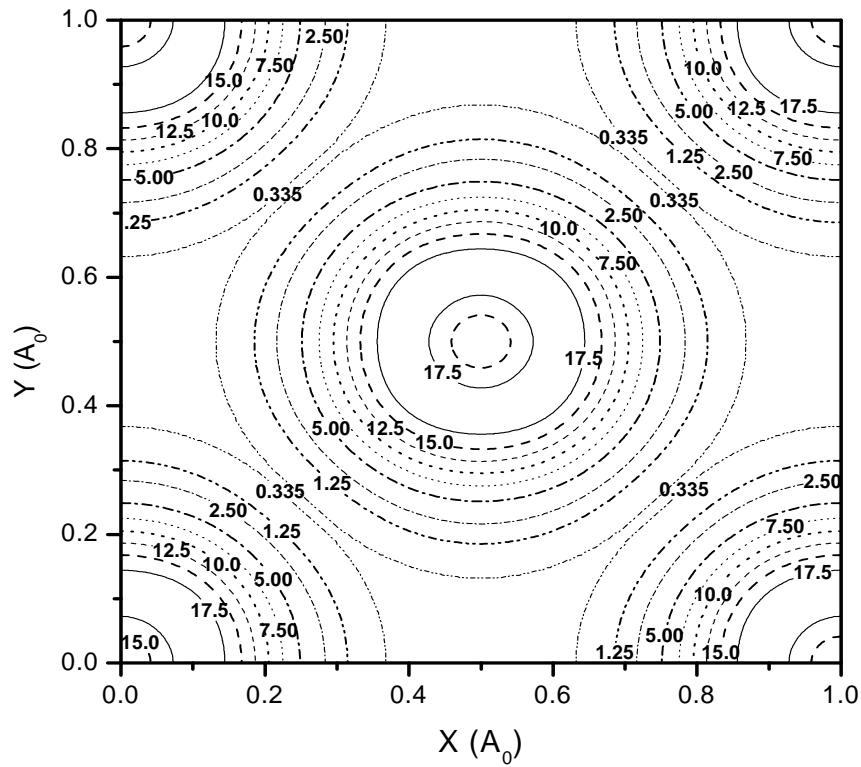


Fig. 2: Electron charge density ($e/a.u.^2$) of valence bands at $z=0.0$ plane for $\text{ZnS}_{0.50}\text{Se}_{0.50}$ at Γ point.

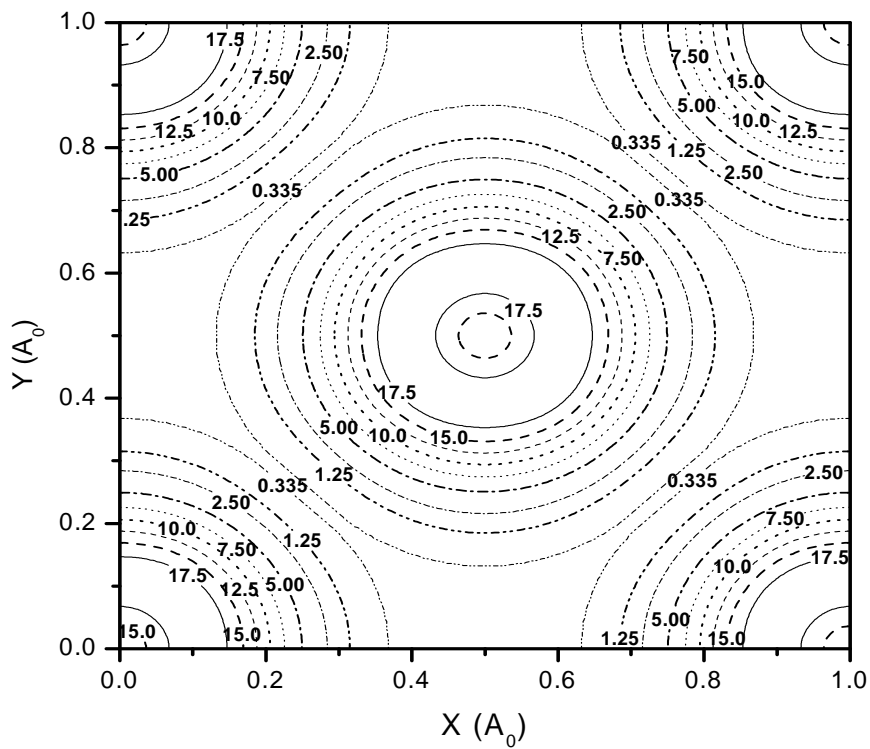


Fig. 3: Electron charge density ($e/a.u.^2$) of valence bands at $z=0.0$ plane for $\text{ZnS}_{0.75}\text{Se}_{0.25}$ at Γ point.

Refractive index (n) is also an important parameter for technological applications of semiconductors. A number of relations have been suggested to estimate n from the computed or measured band gap. In table 2, we give the refractive index determined by means of a number of relations proposed by Moss[34], Herve and Vandamme (HV) [35], and Gupta nad Ravindra (GR) [36]. In the absence of experimental data for alloys comparison can be made only for the binary compounds. It would be better to have experimental estimates of n for all alloys for critical comparison.

3.2 Charge density distribution and ionicity:

The valence charge density distributions along cation, anion and the bond intersecting planes are computed. For the sake of presentation, however, we only give the charge density contours for the $\text{ZnS}_{0.25}\text{Se}_{0.75}$, $\text{ZnS}_{0.5}\text{Se}_{0.5}$ and $\text{ZnS}_{0.75}\text{Se}_{0.25}$ alloys [37]. The valence charge densities computed for $\text{ZnS}_{0.25}\text{Se}_{0.75}$, $\text{ZnS}_{0.5}\text{Se}_{0.5}$ and $\text{ZnS}_{0.75}\text{Se}_{0.25}$ at $z=0.0$ plane containing cations i.e. zinc are plotted in figures 1-3. Figures depict that the estimated relative increment in the planar charge density is 1.7, 2.9, 3.8 and 4.4% for $\text{ZnS}_{0.25}\text{Se}_{0.75}$, $\text{ZnS}_{0.5}\text{Se}_{0.5}$, $\text{ZnS}_{0.75}\text{Se}_{0.25}$ and ZnS (not presented here) respectively. As relative increment in the planar area owing to changes in lattice constant from ZnSe to ZnS is less than 0.2 %. It points that the substitution of S in ZnSe causes charge localization around Zn atomic sites.

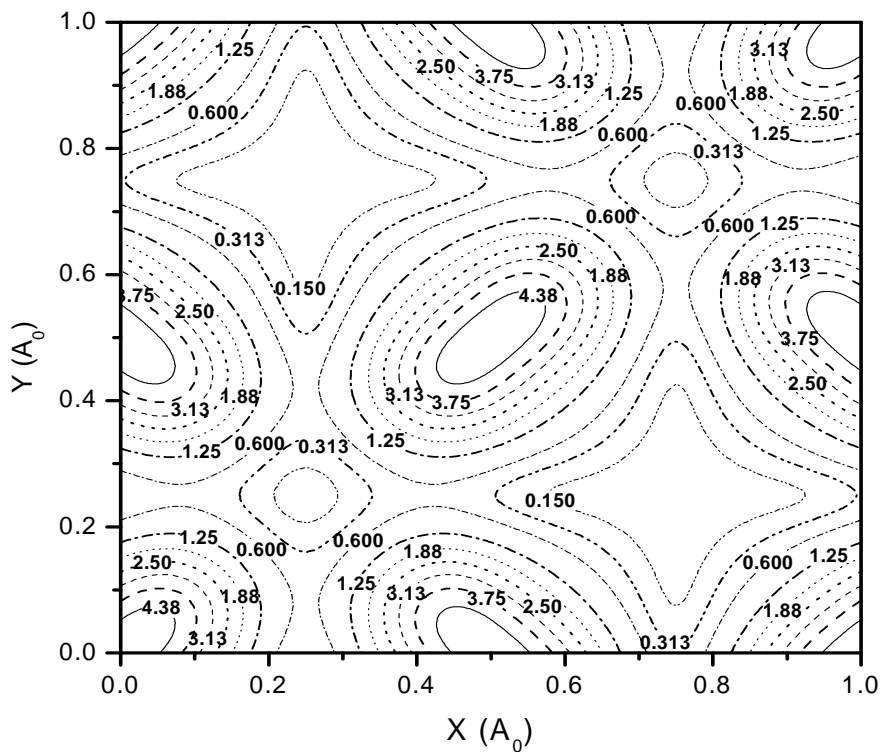


Fig. 4: Electron charge density ($e/a.u.^2$) of valence bands at $z=0.25$ plane for $\text{ZnS}_{0.25}\text{Se}_{0.75}$ at Γ point.

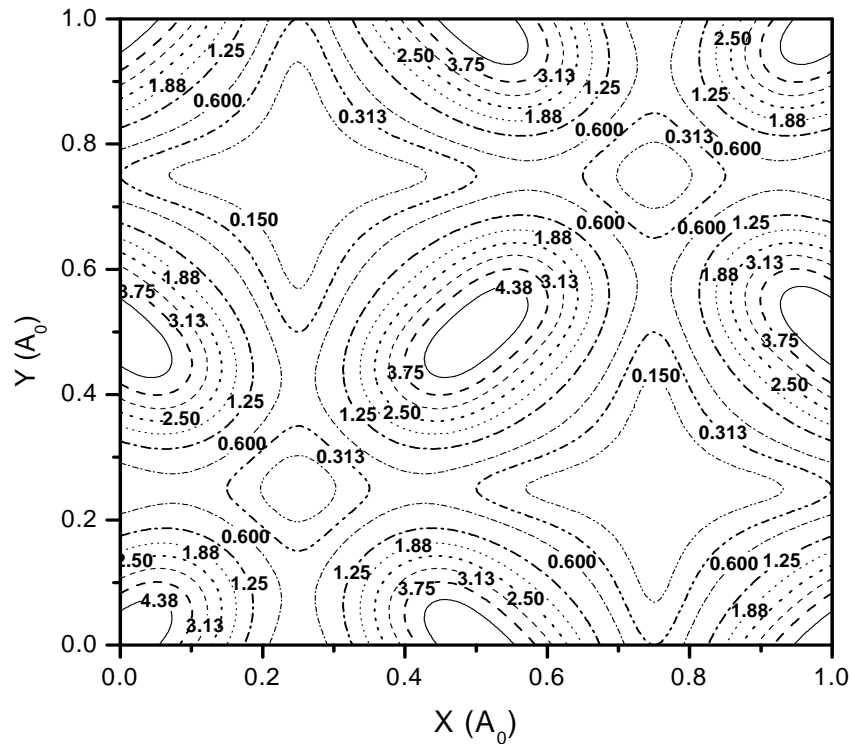


Fig. 5: Electron charge density ($e/a.u.^2$) of valence bands at $z=0.25$ plane for $\text{ZnS}_{0.50}\text{Se}_{0.50}$ at Γ point.

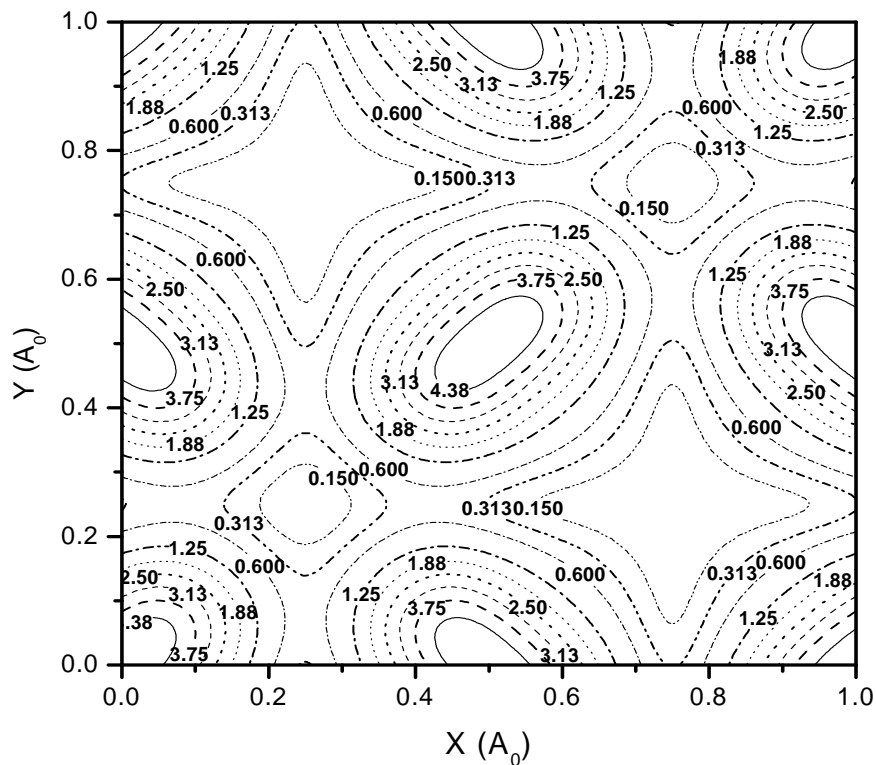


Fig. 6: Electron charge density ($e/a.u.^2$) of valence bands at $z=0.25$ plane for $\text{ZnS}_{0.75}\text{Se}_{0.25}$ at Γ point.

Figures 4 to 6 show calculated valence charge density distribution in the $z=0.25$ plane containing S or Se sites for $\text{ZnS}_{0.25}\text{Se}_{0.75}$, $\text{ZnS}_{0.5}\text{Se}_{0.5}$ and $\text{ZnS}_{0.75}\text{Se}_{0.25}$ alloys respectively. In these alloys, the calculated charge density in the $z=0.25$ plane is higher in the middle of the anion sites.

In the middle, charge density is observed to get localized and localization increases with concentration of S whereas overall planar charge density decreases with S. This indicates that substitution of S results localization of charge in the middle of the anion sites (i.e. S or Se) rather than at the anion sites in the $z=0.25$ plane.

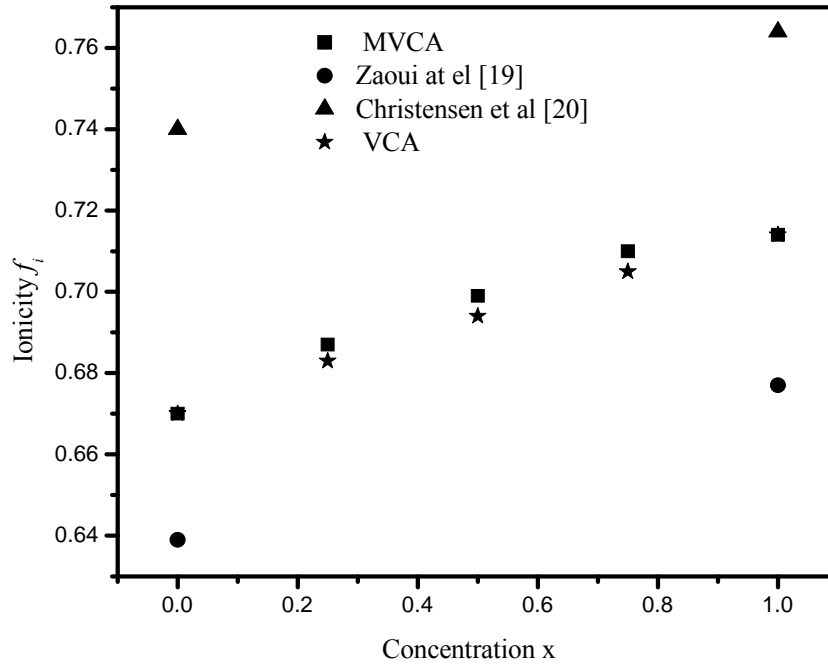


Fig. 7: Ionicity factors for ZnS_xSe_{1-x} alloys deduced from EPM applying VCA and MVCA. Ionicity factors reported by Zaoui et al [27] and Christensen et al [28] for ZnSe and ZnS are also plotted.

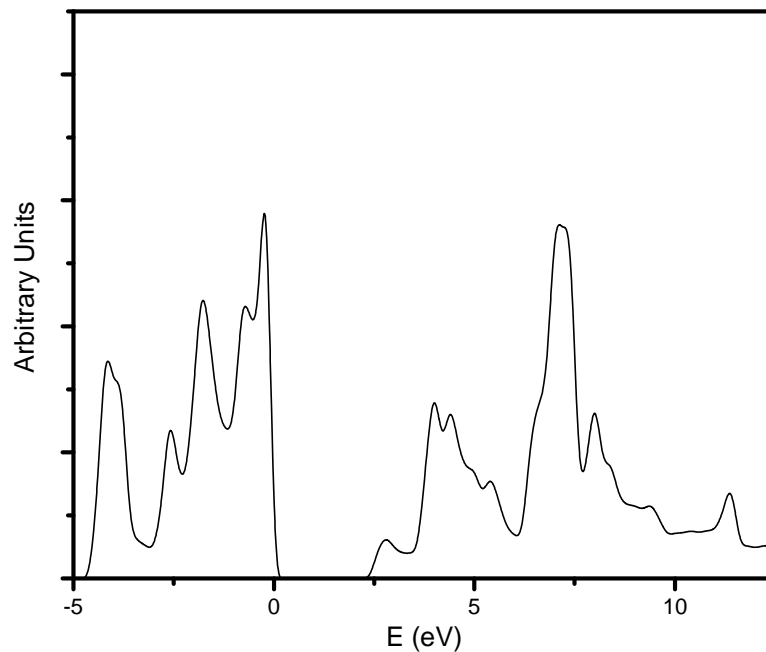


Fig. 8: Total density of states for ZnSe on arbitrary scale. The first valence band lies well below 12.8 eV.

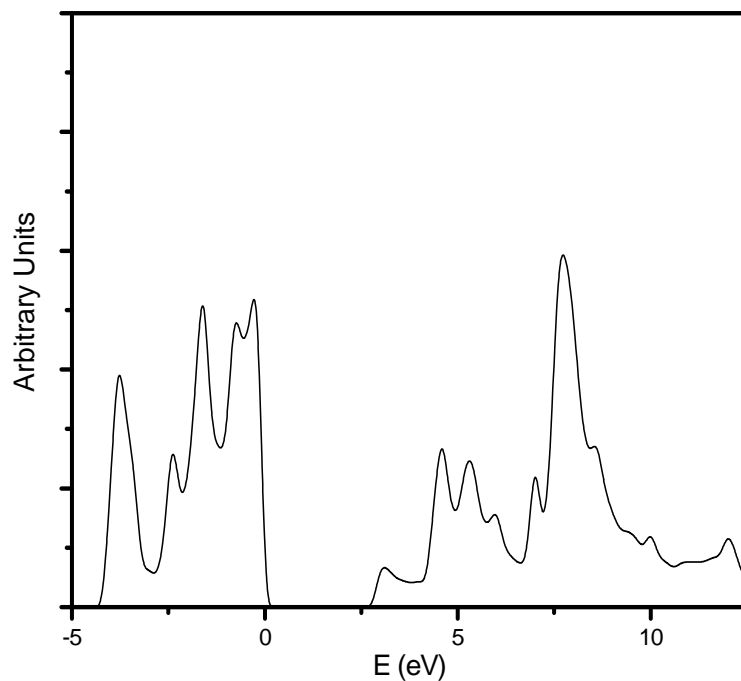


Fig. 9 : Total density of states for $\text{ZnS}_{0.5}\text{Se}_{0.5}$ on arbitrary scale. The first valence band lies well below 12.8 eV.

From figures 1-6, one can also examine the build up of charge density with substitution of S in ZnSe at $z=0.0$ and $z=0.25$ planes. It is visually obvious that the charge density changes and gets reorganized below $x=0.75$ and no substantial changes are seen thereafter for $\text{ZnS}_{0.75}\text{Se}_{0.25}$ and ZnS (not shown here). Charge density distributions for these alloys on the bond intersecting plane, i.e. $z=0.125$, also show similar trends [37].

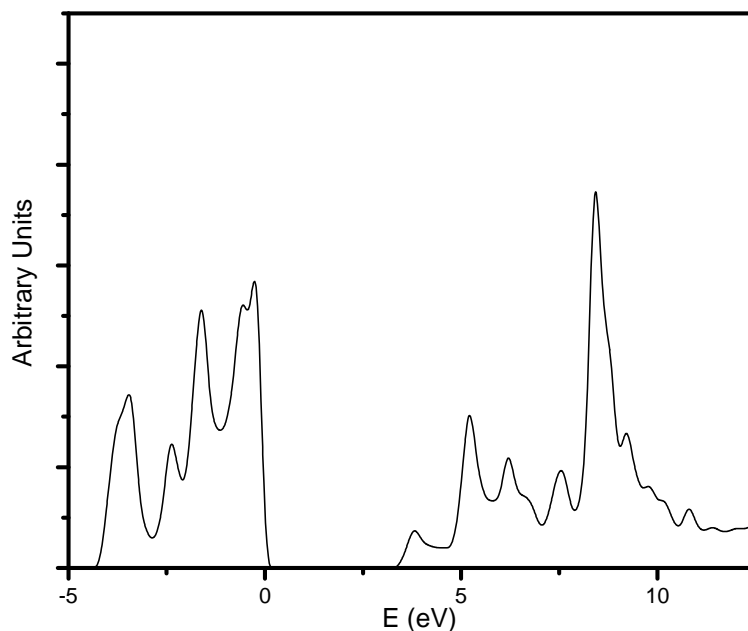


Fig. 10 : Total density of states for ZnS on arbitrary scale. The first valence band lies well below 12.8 eV.

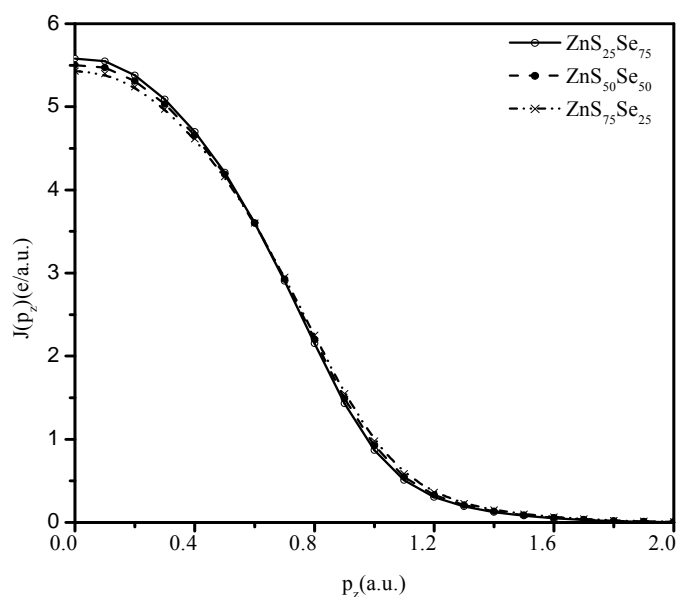


Fig. 11: The valence Compton profiles of $\text{ZnS}_x\text{Se}_{1-x}$ ($x=0.25, 0.5$ and 0.75) alloys.

A close inspection of charge density distributions plotted in figures 1 to 6 reveals that planar charge density increases in the cation plane (i.e. $z=0.0$) and decreases in the anion plane (i.e. $z=0.25$) with composition x . These changes are specifically seen at the atomic sites of the cation and anion. However, no substantial change in the planar charge density in the bond intersecting plane ($z=0.125$) is observed. It clearly points charge transfer from anion to cation plane. The increase in charge transfer without affecting the bond intersecting plane may be attributed to enhancement in ionicity. A similar study on the basis of Mulliken charge population on these alloys might have been fruitful for comparison enabling further critical analysis of these findings. Nevertheless, to quantify the charge transfer we compute the ionicity factor f_i for entire composition range in the interval of 0.25. The heteropolar band gaps obtained using MVCA and VCA are substituted in Eq. (2), as described before, to determine the ionicity factors f_i for all alloys. The ionicity factors f_i computed from our calculations are plotted in Fig. 7. The ionicity factors reported by Zaoui et al [27] and Christensen et al [28] are also plotted in Fig. 7 for comparison. Figure depicts that the ionicity factor computed using MVCA differs from VCA by merely 0.7 percent. All calculations suggest an increasing trend in the ionicity from ZnSe to ZnS. It may be important to emphasize that the calculated ionicity for $\text{ZnS}_x\text{Se}_{1-x}$ is found to be larger than $\text{Ga}_x\text{Al}_{1-x}\text{Sb}$ alloys [20] well in accordance with the findings of Vyas et al [19] who observed larger ionic character in II-VI compounds.

3.3 Density of states

Calculated density of states (DOS) of $\text{ZnS}_x\text{Se}_{1-x}$ for $x=0.0, 0.50$ and 1.0 are plotted in figures 8, 9 and 10. The occupied states below 12.8 eV are entirely contributed by the first valence band in all compositions (not presented in the figures). Figures also show that around 5 eV, the occupied states dominated by the p states are deeper in ZnSe. With the substitution of S states shift towards Valence band maximum. Near valence band maximum, the role of sulfur substitution is seen as broadening the DOS. The effect of substitution of S in ZnSe is largely visible in the unoccupied DOS (UDOS). For $\text{ZnS}_{0.5}\text{Se}_{0.5}$ the peaks of the two bands coalesce to give large number of states. These findings may be examined by performing inverse photoemission measurements and may probably be useful to look into the possibility to grow p-type or n-type doping in $\text{ZnS}_x\text{Se}_{1-x}$ alloys [38].

3.4 Electron momentum density

The electron momentum density $\rho(\mathbf{p})$ is the ground state property of materials. When $\rho(\mathbf{p})$ is integrated over two components of the electron momentum, it gives Compton profile defined as:

$$J(p_z) = \iint \rho(\mathbf{p}) dp_x dp_y. \quad (3)$$

It quantifies occupation of charge in momentum space. It also contains signatures of Fermi surface in metals and behavior of bonding electrons in other materials [21,22]. We computed the directional Compton profiles along six principal directions for all the alloys and thereafter the average Compton profiles are obtained by the formula of Miasek [39]. These average Compton profiles for the three alloys are plotted in Fig. 11. In the low momentum region ($0.0 \leq p_z \leq 0.5$) the profile corresponding to $\text{ZnS}_{0.25}\text{Se}_{0.75}$ is the largest. It is 2.8% larger than the $\text{ZnS}_{0.75}\text{Se}_{0.25}$ whereas the profile corresponding to $\text{ZnS}_{0.5}\text{Se}_{0.5}$ is 1.4% larger than the $\text{ZnS}_{0.75}\text{Se}_{0.25}$. It points that addition of Se in ZnS leads to larger momentum density distribution in the low momentum region ($0.0 \leq p_z \leq 0.5$). The trend gets reversed beyond 0.5 a.u. as a manifestation of the normalization. As measurements are not available for the alloys, on the basis of measurements reported for ZnS and ZnSe [40] one may anticipate these trends in the experimental profiles also. A rigorous comparison can be done only when momentum density distribution measurements on these materials are performed. It is hoped that this work may inspire such work in future.

4. Conclusions

Modified virtual crystal approximation has been employed in the EPM scheme to calculate electronic states, refractive index, charge density, ionicity, density of states and electron momentum densities for the $\text{ZnS}_x\text{Se}_{1-x}$ alloys. It has been observed that:

(i) The calculated band gaps and bowing computed using MVCA are in good agreement with the experiments.

(ii) The refractive indices are proposed for alloys. These may be compared with the measurements to appear in future. For ZnS and ZnSe the Moss and HV relations give estimates of refractive index closer to the experimental data.

(iii) The ionicity factor is found to increase in the $\text{ZnS}_x\text{Se}_{1-x}$ alloys with increase in x . On the basis of charge density calculations the increase in ionicity may be attributed to charge transfer taking place from the cation plane to the anion planes.

(iv) The occupied DOS and the unoccupied DOS show the effect of substitution of S. The effects are largely visible in the UDOS. The present study demands that the experimental probes like inverse photoemission spectroscopy could be fruitful to examine the features in the UDOS rigorously. Then perhaps one may look into the possibility to alter the electronic properties of $\text{ZnS}_x\text{Se}_{1-x}$ alloys by doping. Present study calls for such experiments in future.

(v) Calculations of electron momentum density show that momentum density in the low momentum region increases on adding Se in ZnS. Measurements on end materials support these findings. Similar measurements on alloys are highly required for rigorous comparison.

Acknowledgement

This work is financially supported by the Department of Science and Technology, New Delhi through grant No. SR/S2/CMP-15/2004.

References

- [1] G.F. Neumark, R.M. Park and M. DePuydt, Phys. Today **47**, 26 (1994).
- [2] B. Gil, T. Cloitre, M.D. Blasio, P. Bigenwald, L. Aigouy, N. Briot, O. Briot, D.

- Bouchara, R.L. Aulombard and J. Calas, Phys. Rev. B **50**, 18231 (1994).
- [3] M. Godlewski, E. Guziewicz, K. Kopalko, E. Lusakowska, E. Dynowska, M.M. Godlewski, E.M. Goldys and M.R. Phillips, J. Luminesc. **102**, 455 (2003).
- [4] D. Shen, S.Y. Au, G. Han, D. Que, N. Wang and I.K. Sou, J. Mat. Sci. Lett. **22**, 483 (2003).
- [5] T. Homann, U. Hotje, M. Binnewies, A. Borger, K.-D. Becker and T. Bredow, Solid State Sci. **8**, 44 (2006).
- [6] S.A.B. Nasrallah, N. Sfina, N. Bouarissa and M. Said, J. Phys.: Condens. Matter **18**, 3005 (2006).
- [7] F. Janetzko and K. Jug, J. Phys. Chem. A **108**, 5449 (2004).
- [8] N. Fitzner, A. Kuligk, R. Redner, M. Stadele, S.M. Goodnick and W. Schattke, Phys. Rev. B **67**, 201201 (2003).
- [9] J. Muscat, A. Wander and N.M. Harrison, Chem. Phys. Lett. **342**, 397 (2001).
- [10] J.E. Bernard and A. Zunger, Phys. Rev. B **36**, 3199 (1987).
- [11] D. Theis, phys. stat. sol. (b), **79**, 125 (1977).
- [12] A. Ebina, E. Fukunaka and T. Takahashi, Phys. Rev. B **10**, 2495 (1974).
- [13] R. Dovesi, R. Orlando, C. Roetti, C. Pisani, V.R. Saunders, Phys. Stat. Sol. (b) **217**, 63 (2000).
- [14] M. Rabah, B. Abbar, Y. Al-Douri, B. Bouhafis and B. Saharaoui, Mater. Sci and Engg. B **100**, 163 (2003).
- [15] A. Di Carlo, Semicond. Sci. Technol. **18**, R1 (2003).
- [16] G.C. Dente and M.L. Tilton, J. Appl. Phys. **86**, 1420 (2003).
- [17] A. Ben Fredj, M. Debbichi and M Said, Microelec. Jour. **38**, 860 (2007).
- [18] X. Liu, and J.K. Furdyna, J. Appl. Phys. **95**, 7754 (2004).
- [19] V. Vyas, V. Purvia, Y.C. Sharma, K.B. Joshi and B.K. Sharma, Phys. Stat. Sol. (b) **243**, 1253 (2006).
- [20] K.B. Joshi and N. N. Patel, Pramana- J. Phys. **70**, 295 (2008).
- [21] *X-ray Compton scattering* eds. M.J. Cooper, P.E. Mijnarends, N. Shiotani, N.Sakai and A. Bansil (Oxford Publishing Press, 2004).
- [22] S. Berko, in *Compton Scattering* ed. B. Williams (McGraw-Hill Publishing, London 1977).
- [23] M.L. Cohen and J. R. Chelokowsky, in *Electronic structure and properties of Semiconductors*, edited by M. Cordona (Springer, Berlin, 1988) Vol.75.
- [24] A. Bechiri, F. Benmakhlof and N. Bouarissa, Mater. Chem. Phys. **77**, 507 (2003).
- [25] F. Long, P. Harrison and W.E. Hagston, J. Appl. Phys., **79(9)**, 6939 (1996).
- [26] Y. Al-Douri, R. Khenata, Z. Chelahi-Chikr, M. Driz and H. Aourag; J. Appl. Phys. **94**, 4502 (2003).
- [27] A. Zaoui, M. Ferhat, B. Khelifa, J.P. Dufour, H. Aourag, Phys. Stat. Sol. (b) **185**, 163 (1994).
- [28] N.E. Christensen, S. Satpathy and Z. Pawlowska, Phys. Rev. **B36**, 1032 (1987).
- [29] L. Vegard, Z. Phys. **5**, 17 (1921).
- [30] P. Pattison, N.K. Hansen and J.R. Schneider, Chem. Phys. **59**, 231 (1981).
- [31] D.J. Chadi and M.L. Cohen, Phys. Rev. **B8**, 5747 (1973).
- [32] C.G. Van de Walle, Phys. Rev. **B39**, 1871 (1989).
- [33] J.E. Nicholls, J.J. Davies, N.R. Podton, R. Mach and G.O. Mullar, J. Phys. Chem. **18**, 455 (1985).
- [34] T. S. Moss, Proc. Phys. Soc. London B **63**, 167 (1950).
- [35] P. Herve and L.K.J. Vandamme, Infrared Phys. Technol. **35**, 609 (1994).
- [36] V.P. Gupta and N.M. Ravindra, Phys. Stat. Sol. (b) **100**, 715 (1980).
- [37] Those charge density contours which are not presented as figures can be obtained from authors on request.
- [38] N. Tit, J. Phys. D: Appl. Phys. **36**, 961 (2003).
- [39] M. Miasek, J. Math. Phys. **7**, 139 (1966).
- [40] B.K. Panda and H.C. Padhi, Phys. Stat. Sol.(b) **166**, 519 (1991).
- [41] D.W. Palmer @ www.semiconductor.co.uk.